THE JOURNAL OF BIOLOGICAL CHEMISTRY VOL. 284, NO. 50, pp. 34998–35014, December 11, 2009

Loss of Myosin VI No Insert Isoform (NoI) Induces a Defect in Clathrin-mediated Endocytosis and Leads to Caveolar Endocytosis of Transferrin Receptor*[S]

Received for publication, April 23, 2009, and in revised form, September 18, 2009 Published, JBC Papers in Press, October 18, 2009, DOI 10.1074/jbc.M109.012328

Claudia Puri[1]

From the Cambridge Institute for Medical Research, University of Cambridge, Wellcome Trust/MRC Building, Hills Road, Cambridge CB2 2XY, United Kingdom

Myosin VI is a motor protein that moves toward the minus end of actin filaments. It is involved in clathrin-mediated endocytosis and associates with clathrin-coated pits/vesicles at the plasma membrane. In this article the effect of the loss of myosin VI no insert isoform (NoI) on endocytosis in nonpolarized cells was examined. The absence of myosin VI in fibroblasts derived from the Snell's waltzer mouse (myosin VI knock-out) gives rise to defective clathrin-mediated endocytosis with shallow clathrin-coated pits and a strong reduction in the internalization of clathrin-coated vesicles. To compensate for this defect in clathrin-mediated endocytosis, plasma membrane receptors such as the transferrin receptor (TfR) are internalized by a caveola-dependent pathway. Moreover the clathrin adaptor protein, AP-2, necessary for TfR internalization, follows the receptor and relocalizes in caveolae in Snell's waltzer fibroblasts.

In eukaryotic cells diverse endocytic uptake pathways occur at the plasma membrane; these have crucial roles in signal transduction, immune surveillance, antigen presentation, cell-cell communication, and cellular homeostasis. Clathrin-mediated endocytosis is by far the best characterized pathway by which cells internalize protein and lipid molecules, although at least three other basic mechanisms, caveola-mediated endocytosis, macropinocytosis, and clathrin- and caveola-independent endocytosis, are also known to operate (1, 2). Recent results have suggested that signaling receptors such as epidermal growth factor receptor (EGFR)[2] and other receptor tyrosine kinases could be endocytosed not only by the clathrin-dependent pathway but also by alternative pathways involving circular dorsal ruffles (3) or by caveolin/raft-dependent endocytosis (4–7). Moreover, it was recently observed that the transferrin receptor (TfR), a nonsignaling receptor that is internalized canonically by clathrin-mediated endocytosis, can also be endocytosed by a clathrin/dynamin-independent, cholesterol-dependent pathway (8).

Caveolae were first observed more than 50 years ago on the surface of endothelial cells; caveola-mediated endocytosis is the best described clathrin-independent uptake route. Caveolae, flask-shaped invaginations of the plasma membrane, are specialized lipid raft domains that are rich in cholesterol and sphingolipids, with shape and structural organization maintained by the integral membrane protein caveolin. Although not all mammalian cells express caveolin, caveolae are very abundant at the plasma membrane of fibroblasts, adipocytes, and endothelial and smooth muscle cells; however, the precise uptake mechanism involved and how it is triggered and regulated are thus far rather poorly understood.

Motor proteins such as myosin VI have been shown to be involved in clathrin-mediated endocytosis (9–13). Myosin VI is a unique actin-based motor protein that moves toward the minus end of actin filaments, in the opposite direction to all other myosins characterized thus far (14). In mammalian cells, four alternatively spliced myosin VI isoforms have been identified that contain, in the tail region, no insert (NoI), a small insert (SI; 9 amino acids), a large insert (LI; 21–31 amino acids), or both the small and large inserts (S+L). The large insert isoform is expressed in polarized cells at the apical domain, whereas the NoI and the SI are expressed either in basolateral or apical domains (15). Moreover, the NoI isoform is expressed in almost all unpolarized cell (9, 16).

The endogenous myosin VI LI isoform in polarized Caco2 cells is associated with clathrin-coated structures at the apical domain (9), but in other cell lines expressing the LI isoform, such as ARPE-19 cells, myosin VI does not co-localize with clathrin (17) or the clathrin adaptor protein, AP-2 (16). When the LI isoform tail, which works as a myosin VI dominant negative inhibitor, is expressed in nonpolarized cells, it is able to localize to clathrin-coated structures but gives rise to a defect in transferrin receptor endocytosis (9). Overexpressing the myosin VI tail in ARPE-19 cells affects the TfR endocytic route (17). The full-length myosin VI NoI splice isoform shows reduced targeting to clathrin-coated structures in nonpolarized rat fibroblast (NRK) cells and in the ARPE-19 cell line and a reduced ability to bring the uncoated vesicles out of the plasma membrane actin-rich region (17). Both myosin VI LI and NoI isoforms are, however, able to bind the endocytic protein Disabled-2 (Dab2) (10). Dab2 is considered an endocytic adaptor protein because it displays

* This work was supported by Cancer Research UK.
[S] The on-line version of this article (available at http://www.jbc.org) contains supplemental Figs. 1 and 2.
[1] To whom correspondence should be addressed. Tel.: 44-1223-336782; Fax: 44-1223-762640; E-mail: cp344@cam.ac.uk and puri@tigem.it.
[2] The abbreviations used are: EGFR, epidermal growth factor receptor; NoI, no insert isoform; SI, small insert; LI, large insert; Tf, transferrin; TfR, transferrin receptor; PIP_2, phosphatidylinositol 4,5-bisphosphate; AMPA, α-amino-3-hydroxy-5-methyl-4-isoxazolepropionic acid; CCS, clathrin-coated structure(s); EM, electron microscopy; C8-LacCer, D-lactosyl-β1-1′-*N*-octanoyl-D-*erythro*-sphingosine; KD, knockdown; TIRF, total internal reflection fluorescence; siRNA, small interfering RNA; GFP, green fluorescent protein; HRP, horseradish peroxidase; PBS, phosphate-buffered saline.

two DPF amino acid motifs, which are able to bind to the clathrin adaptor protein, AP-2 (10, 18). All myosin VI isoforms are recruited to clathrin-coated structures in cells that overexpress Dab2 (16). The recruitment and targeting of myosin VI to clathrin-coated structures at the plasma membrane require that Dab2 binds to the WWY sequence motif, and phosphatidylinositol 4,5-bisphosphate (PIP_2) binds to the WKSKNKKR region in the C-terminal cargo-binding domain of myosin VI (12). These binding sites are conserved in all myosin VI isoforms. In fact when the myosin VI NoI or LI isoform tails are transfected into NRK cells, both isoforms are targeted to clathrin-coated structures (16). PIP_2 is also able to bind Dab2 and clathrin adaptor protein AP-2 directly (19, 20). Myosin VI has a number of different functions in membrane trafficking, such as the sorting and delivering of AP-1B-dependent cargo to the basolateral domain in polarized Madin-Darby canine kidney cells (15) and the transport of transferrin receptor to the endocytic recycling compartment (21, 22).

In the Snell's waltzer mouse (sv/sv; the myosin knock-out) an intragenic deletion of the *Myo6* gene results in a complete lack of myosin VI expression (23). The most obvious phenotype in the sv/sv mouse is an inner ear defect resulting in circling, head tossing, deafness, and hyperactivity (24). Lack of myosin VI in the sv/sv mouse gives rise to degeneration and fusion of the stereocilia in cochlea hair cells (25), whereas in hippocampal neurons there are defects in AMPA receptor endocytosis that result in altered synapse structure and astrogliosis (26). In addition in the apical domain of enterocyte brush border cells, there is a defect in the endocytosis of the cystic fibrosis transmembrane conductance regulator (27). In humans a missense mutation in the myosin VI gene was recently identified in an Italian family with a nonsyndromic dominant form of deafness (28). This C442Y mutation in the motor domain is close to the ATP binding pocket and dramatically increases the rate of ADP dissociation (29). Several different mutations in the myosin VI gene have also been identified in three Pakistani families suffering from recessive deafness (30).

The relatively mild phenotypes observed in the sv/sv mouse are in sharp contrast to the apparently essential roles that myosin VI appears to play in many intracellular processes, especially its crucial role in clathrin-mediated endocytosis. Therefore, to determine how the sv/sv mouse is able to compensate for the lack of myosin VI, the endocytic pathway followed by the TfR (the prototype receptor internalized by clathrin-mediated endocytosis) was studied in sv/sv fibroblasts. In these fibroblasts a significant defect in clathrin-coated vesicle formation and a relocalization of the TfR from clathrin-coated structures (CCS) to caveolae were observed. Clathrin-mediated endocytosis was rescued in these sv/sv fibroblasts by expressing a full-length myosin VI NoI isoform construct. Recruitment of the TfR into caveolae was also observed in siRNA myosin VI knockdown (KD) HeLa cells, in cells overexpressing the dominant negative myosin VI tail, and in human fibroblasts expressing a myosin VI mutant with altered motor properties. In HeLa cells depleted of both myosin VI and caveolin-1, transferrin internalization was inhibited. These results suggest that loss of myosin VI gives rise to a severe defect in clathrin-mediated endocytosis, and to compensate for this defect, alternative endocytic pathways are up-regulated to allow plasma membrane receptors such as the transferrin receptor to be internalized and follow their normal endocytic route. In this scenario, the clathrin adaptor protein, AP-2, necessary for transferrin receptor internalization, is also relocalized to caveolae.

EXPERIMENTAL PROCEDURES

Antibodies and Reagents

The antibodies used were as follows: rabbit anti-myosin VI (Sigma), rabbit anti-myosin VI (C-terminal), and rabbit anti-myosin VI (tail) (gifts from Folma Buss); rabbit anti-caveolin-1 (Santa Cruz Biotechnology, Santa Cruz, CA); rabbit anti-caveolin-1 (BD Biosciences); mouse anti-AP-2 (Affinity BioReagents, Golden, CO); rabbit anti-GFP (Molecular Probes, Eugene, OR); mouse anti-TfR (Zymed Laboratories Inc., San Francisco, CA); mouse anti-TfR 5E9C11 (ATCC, Manassas, VA); rabbit anti-mouse (Dako, Glostrup, Denmark); mouse anti-clathrin (Abcam); human Tf-Alexa-555 (Invitrogen); human Tf-HRP (Jackson ImmunoResearch); and protein A-gold (Cell Microscopy Centre, Utrecht, The Netherland). Filipin, Dynasore, water-soluble cholesterol, and fatty acid-free bovine serum albumin were from Sigma. D-Lactosyl-β1–1′-*N*-octanoyl-D-*erythro*-sphingosine (C8-LacCer) was from Avanti Polar Lipids. Secondary fluorochrome-labeled antibodies were from Molecular Probes. The HeLa cell line stably expressing myosin VI NoI tail and clathrin-GFP light chain were gifts from Folma Buss.

Mouse Fibroblasts

Snell's waltzer (sv/sv) and wild type (wt/wt) mouse fibroblasts were obtained from adult mice using the following procedure. 1 cm of mouse tail was disinfected with ethanol, cut, and placed in a mixture of Dulbecco's modified Eagle's medium supplemented with 10% fetal bovine serum, penicillin (1000 units/ml)/streptomycin (1 mg/ml), and L-glutamine (2 mM). The derma was scraped, homogenized with a 25-gauge needle, and cultured in a 5-cm Petri dish in the same medium described above. Primary fibroblasts were subcultured at low density with medium supplemented with 20% serum to obtain stable clones. The same procedure was performed for wt/wt and myosin VI C442Y mutant human fibroblasts to obtain stable cell lines.

EM Methods

Immunogold Labeling on Cryosections—Mouse and human fibroblasts or HeLa cells were fixed for immunoelectron microscopy with a mixture of 2% paraformaldehyde and 0.2% glutaraldehyde in PBS for 2 h at room temperature. Cells were then prepared for ultrathin cryosectioning and immunogold-labeled according to the protocol described previously (4). The sections were observed in a Philips CM100 transmission electron microscope. Following the normal Epon embedding technique, mouse fibroblasts were fixed in growing condition. The cells were fixed and embedded following the procedure described previously (31). Ruthenium red fixation was performed using a method described previously (31, 32).

Morphometry—Morphometric analysis of immunogold labeling was performed at a magnification of ×10,500 on randomly selected cells profiles with the nucleus for each experiment. Ten random cell profiles were counted for each condition. Clathrin-coated structures were identified directly by the dark shadow of the clathrin coating, whereas caveolae were identified by caveolin-1 labeling. Quantitation of the amount of clathrin-coated structures or caveolae was normalized for a 1000-μm length of cell perimeter. The cell profiles were calculated on low magnification pictures by the "intersection method" (33). The histograms show the percentage of TfR (calculated from the number of gold particles) present on labeled caveolae or clathrin-coated structures (Figs. 5–8). Further details of each experiment are given in the figure legends (Figs. 5–8).

HRP and Tf-HRP Uptake

HRP and Tf-HRP uptake was performed as described previously (34–37). Briefly, the cells were grown on 35-mm dishes, serum-starved for 1 h, washed twice in PBS/$Ca^{2+}Mg^{2+}$, and incubated with 4 mg/ml HRP or 30 μg/ml Tf-HRP for different time periods (5–20 min) at 37 °C in a continuous uptake assay. After the 37 °C uptake, all of the dishes were placed on ice, treated for 10 min with PBS/0.1% Pronase as the stripping/detaching agent, and solubilized in PBS/0.5% Triton X-100. The cell lysates were incubated in the dark for 20 min with 3,3′,5,5′-tetramethylbenzidine. The reaction was stopped with 1 M H_2SO_4, and absorbances were read at 450 nm. The Tf-HRP data were expressed as percentage of the amount of plasma membrane (34). The HRP data were normalized for protein concentrations using the BCA protein assay and expressed as arbitrary units. All experiments were performed in duplicate.

Pharmacological Studies

Dynasore, filipin, filipin/cholesterol, and C8-LacCer treatments were performed using methods described previously (4, 38–40). Briefly, wt/wt and sv/sv fibroblasts were starved for 1 h in serum-free medium and incubated for 1 h with filipin (1.2 μg/ml), filipin/cholesterol (1.2 μg/ml-1 mM), Dynasore (120 mM), and C8-LacCer (10 μM) followed by incubation with Tf-HRP in continuous uptake for 5 min. The cells were then treated as described above.

Gene Silencing

HeLa cells were transfected twice with human myosin VI or/and caveolin-1 ON-TARGETplus SMARTpool siRNAs (Dharmacon) using Oligofectamine (Invitrogen) as described previously (41). The mock cells were transfected either with a control siRNA such as a scrambled oligo or with Oligofectamine only. Western blot analysis was used to check the level of myosin VI/caveolin-1 in these cells. HeLa stable cell lines that down-regulate myosin VI were obtained with SureSilencing™ myosin VI small hairpin RNA plasmids (SuperArray-Bioscience Corp.) according to the manufacturer's instructions.

sv/sv MVI NoI

The GFP-tagged full-length myosin VI NoI isoform was cloned into the PIRESneo vector (Invitrogen) and transfected into sv/sv mouse fibroblasts using FuGENE (Roche Applied Science). Stable sv/sv mouse fibroblasts cell lines were selected with 500 μg/ml G418 (Invitrogen). A plug of individual clones for each construct was grown in selective medium, and the population of highly expressing cells was enriched by fluorescence-activated cell sorting.

PCR Analysis

To assess the expression of myosin VI in HeLa cells and in human and in mouse fibroblasts, the Purescript® RNA isolation kit was used (Gentra Systems). The resulting RNAs were used in reverse transcription-PCR reactions using primers flanking the myosin VI tail region. The expression levels of the different myosin VI isoforms were visualized by running the PCR products on agarose gels.

Immunofluorescence

HeLa cells, mock or expressing GFP-myosin NoI isoform or GFP-myosin VI NoI tail, were fixed with 4% paraformaldehyde, permeabilized with 0.1% Triton, blocked with 1% bovine serum albumin in PBS, and processed for indirect immunofluorescence using rabbit anti-myosin VI or rabbit anti-GFP and mouse anti-AP-2 followed by secondary antibodies coupled with Alexa-488 or Alexa-555. Snell's waltzer and wt/wt fibroblasts were incubated for 15 min at 37 °C with Tf-Alexa-555 (25 μg/ml). The cells were washed twice with PBS, fixed with 4% paraformaldehyde in PBS, and labeled with anti-AP-2 antibody, clathrin, and caveolin-1. The cells were visualized with a Zeiss Axioplan epifluorescence microscope, a Zeiss LSM-510 confocal microscope, or a Zeiss TIRF 3 microscope (Carl Zeiss MicroImaging Inc.). wt/wt and sv/sv fibroblasts were transfected with clathrin-GFP light chain and analyzed by total internal reflection fluorescence (TIRF) microscopy (TIRF 3, Carl Zeiss MicroImaging Inc.). 500 fields of 150 × 150 pixels were analyzed by Volocity software, version 5 (Improvision-PerkinElmer).

Western Blot Analysis

wt/wt and sv/sv fibroblasts or HeLa cells in steady state conditions were lysated directly in SDS-sample buffer and analyzed by SDS-PAGE followed by immunoblotting. Blots were developed using ECL detection reagent (Amersham Biosciences).

RESULTS

The Myosin VI NoI Isoform Is Targeted to CCS at the Plasma Membrane—To investigate the role of myosin VI in clathrin-mediated endocytosis at the ultrastructural level, skin fibroblasts were isolated from wild type and Snell's waltzer mice that lack myosin VI. Primary fibroblasts were cultured for several weeks to generate spontaneous immortalized cell lines. Using a PCR-based strategy, we established that in nonpolarized human fibroblasts and HeLa cells, only the myosin VI NoI isoform was expressed, whereas in mouse fibroblasts we detected both NoI and myosin VI SI isoforms (Fig. 1*A*). Previous studies had shown that in NRK cells the myosin VI LI isoform is recruited with high affinity to CCS at the plasma membrane, whereas the endogenous myosin VI NoI isoform shows only partial co-localization with clathrin (9). In a HeLa cell line over-

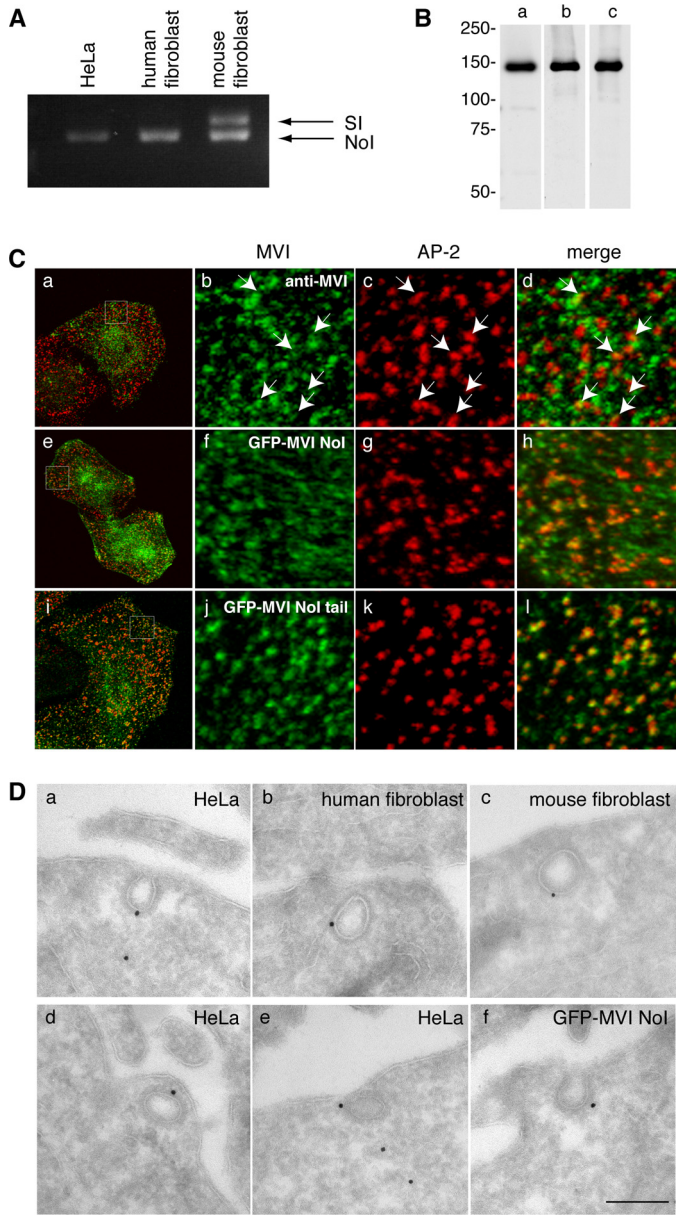

FIGURE 1. **The myosin VI NoI isoform localizes to CCS at the plasma membrane.** *A*, PCR analysis of myosin VI isoforms expressed in nonpolarized cells. HeLa cells and human wild type fibroblasts express the myosin VI NoI isoform, whereas mouse wild type fibroblasts express both the NoI and the SI isoforms. *B*, Western blot analysis of HeLa whole cell lysates using different myosin VI antibodies: an antibody against the C-terminal tail (*lane a*), an antibody against the whole tail (*lane b*), and the C-terminal tail of myosin VI (*lane c*). *C*, co-localization of myosin VI (*a–d*), GFP-myosin VI NoI (*e–h*), and GFP-myosin VI NoI tail (*i–l*) with AP-2. The *boxes* in the merged image in *a*, *e*, and *i* indicate the areas enlarged in the adjacent panels *b–d*, *f–h*, and *j–l*, respectively. *Arrows* indicate examples of co-localization. *D*, to visualize myosin VI localization at the ultrastructural level in unpolarized cells, cryosections of HeLa cells and human and mouse wild type fibroblasts were immunogold-labeled with a commercial antibody to the C-terminal region of myosin VI (*a–c*), an antibody to the whole tail (*d*), or an antibody the C-terminal tail of myosin VI (*e*). Cryosections of HeLa cells expressing GFP-myosin VI NoI were labeled with an antibody against GFP (*f*). *Bars*: *a*, 200 nm; *b*, 200 nm; *c*, 300 nm; *d*, 200 nm; *e*, 200 nm; *f*, 200 nm.

expressing either full-length GFP-myosin VI NoI or GFP-myosin VI NoI tail, a significant increase in the number of AP-2 positive structures containing full-length myosin VI NoI or only the NoI tail were observed compared with the endogenous myosin VI (Fig. 1*C*). The NoI tail domain is targeted to clathrin-coated structures, but without a functional motor domain it cannot be released again, which results in the increased co-localization of the NoI tail with AP-2 (Fig. 1*C*, *i–l*). Similar results were obtained in wild type (wt/wt) mouse fibroblasts for the endogenous myosin VI and overexpressing full-length myosin VI NoI or the NoI tail (supplemental Fig. 1). In HeLa and mouse fibroblasts there is only a small amount of co-localization of the endogenous myosin VI with AP-2, but it is specific, as demonstrated in the experiments shown in supplemental Fig. 2. Endogenous myosin VI was detected at the ultrastructural level in clathrin-coated pits and vesicles in HeLa cells and in human and mouse fibroblasts using a range of different polyclonal antibodies against myosin VI (Fig. 1, *B* and *D*, *a–e*), whereas in the HeLa cell line expressing full-length GFP-myosin VI NoI, its localization was detected using a polyclonal antibody to GFP (Fig. 1*D*, *f*).

The specificities of the myosin VI antibodies used are shown in a Western blot (Fig. 1*B*). These results demonstrate that the myosin VI NoI isoform, which is the isoform expressed in nonpolarized cells, can be recruited to clathrin-coated structures at the plasma membrane.

Analysis of Clathrin-coated Structure Profiles in Snell's Waltzer Fibroblasts—Previous studies on sv/sv mice have shown that the absence of myosin VI leads to a reduction in AMPA receptor endocytosis in hippocampal neurons (26) and a defect in cystic fibrosis transmembrane conductance regulator internalization in enterocytes (27). However it is not known whether other ubiquitous plasma membrane receptors such as TfR are internalized normally in the absence of myosin VI. So to compare clathrin-coated pit and vesicle formation at the ultrastructural level in sv/sv and wt/wt fibroblasts, they were fixed and embedded in Epon, and sections were cut and analyzed by EM. sv/sv fibroblasts showed mostly flat, shallow, clathrin-coated pit profiles at the plasma membrane and few clathrin-coated vesicle profiles (clathrin-coated structures with no connection with the plasma membrane). Representative micrographs of wt/wt and sv/sv fibroblasts are shown in Fig. 2*A*. To quantify this observation, a morphometric analysis from four independent experiments was performed. Cross-sections of CCS were divided into shallow clathrin-coated pits (*panel I*), invaginated clathrin-coated pits (*panel II*), and clathrin-coated structures without an obvious connection with the plasma membrane, which can be either a pit or a vesicle (*panel III*) (Fig. 2*B*). The number of CCS profiles in each category for wt/wt and sv/sv fibroblasts are summarized in the *table* in Fig. 2*B*. The results show that in sv/sv fibroblasts more shallow clathrin-coated pits (I) (53%) and less pit/vesicles (III) (16%) are present compared with wt/wt fibroblasts, where 25% shallow pits (I) and 49% of pit/vesicles (III) were observed. Moreover the total number of clathrin-coated structure profiles (per 1000 μm of cell perimeter) in the sv/sv cells is less than in the wt/wt cells (6 *versus* 8.8) (Fig. 2*C*). These observations at the ultrastructural level suggest that in sv/sv fibroblasts less clathrin-coated structures are assembled, and those that are assembled are mostly shallow clathrin-coated pits. To further investigate whether sv/sv fibroblasts show less clathrin-coated structures than wt/wt, mouse fibroblasts (sv/sv and wt/wt) were transfected with clathrin-GFP light chain and analyzed by TIRF

A

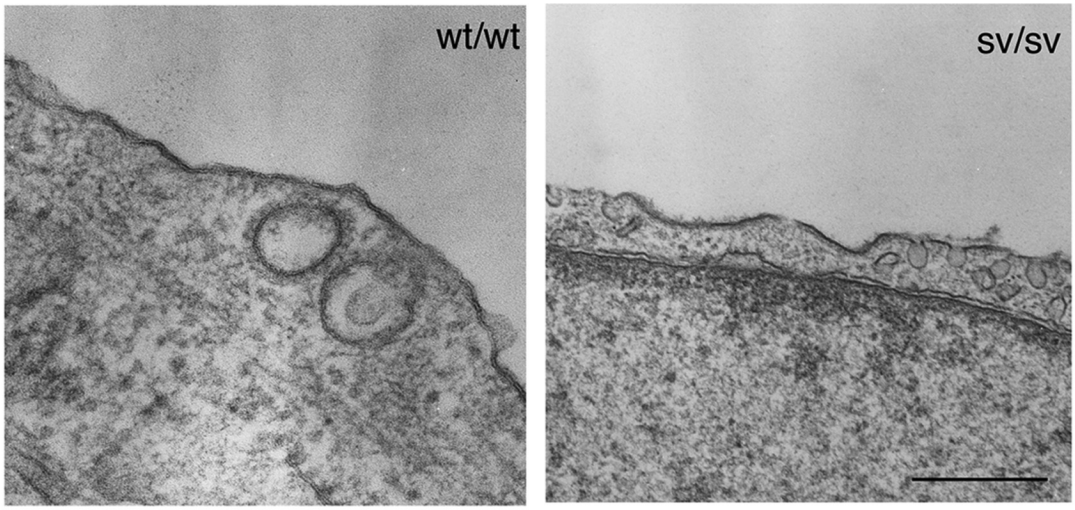

B

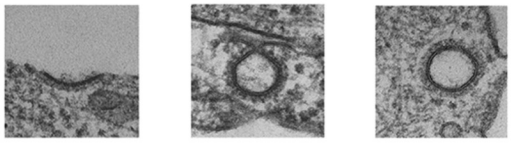

	I	II	III
wt/wt	2.1 ± 0.3	2.3 ± 0.7	4.4 ± 1.5
sv/sv	3.2 ± 1.5	1.7 ± 0.6	1.1 ± 0.5

I: shallow clathrin coated pit
II: invaginated clathrin coated pit
III: clathrin coated pit or vesicle

C

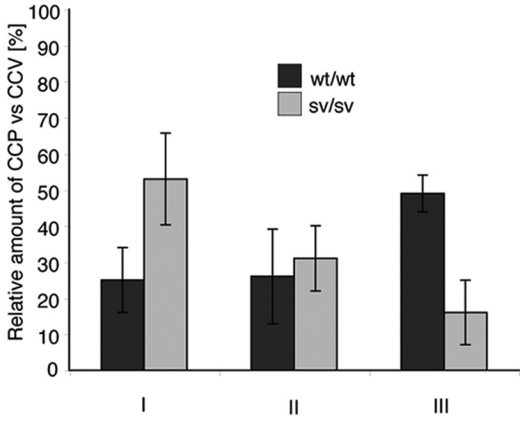

D

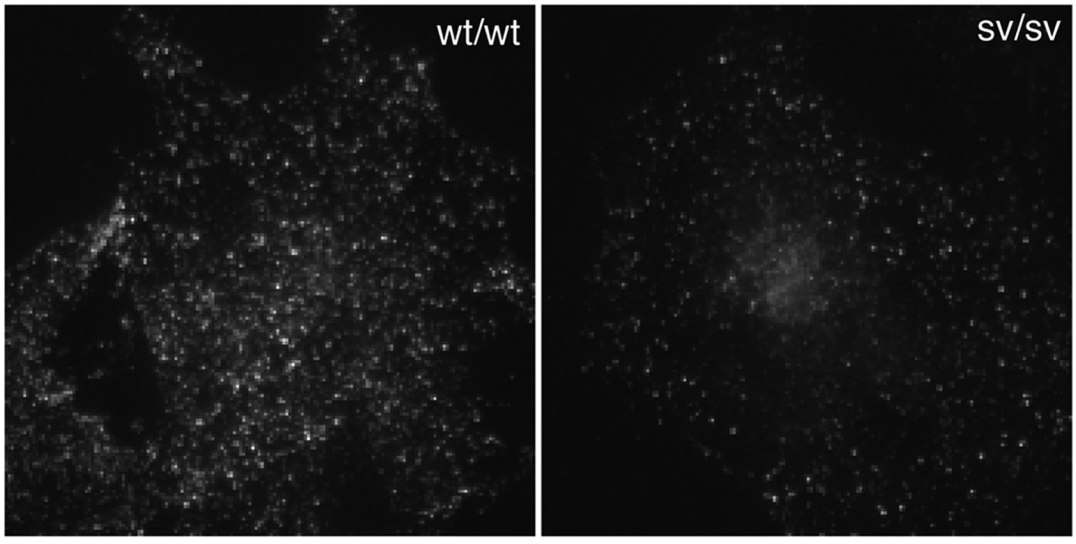

E

	Clathrin-GFP
wt/wt	162 ±4
sv/sv	91 ±3

microscope. A decrease of clathrin positive structures also was observed in sv/sv fibroblasts compared with wt/wt (Fig. 2, *D* and *E*).

sv/sv Fibroblasts Show a Dramatic Decrease in Clathrin-coated Vesicle Formation—The ultrastructural analysis of sv/sv fibroblasts indicated that these cells contained fewer cross-sections of clathrin-coated structures without a visible connection to the plasma membrane. These structures could either be a "real vesicle" that has pinched off from the plasma membrane or a transverse section of a pit, which does not show a connection with the plasma membrane. To distinguish between a pit and a vesicle profile, we analyzed cells fixed in the presence of ruthenium red. This dye is deposited as a dark fuzzy layer on the outside of the plasma membrane and on membrane invaginations still connected with the cell surface, but it is not present on intracellular membranes. Therefore fixing wt/wt and sv/sv fibroblasts in the presence of ruthenium red allowed us to distinguish between a clathrin-coated pit and an internalized clathrin-coated vesicle (Fig. 3*A*). These experiments were performed using one wild type fibroblast cell line and two different Snell's waltzer cell lines derived from two different mice. Analysis and quantization of 100 CCS (from two independent experiments; $n = 2$) fixed with ruthenium red revealed that in wild type fibroblasts 65% of the CCS were pits and 35% were internalized clathrin-coated vesicles without ruthenium red staining (Fig. 3*B*). In sv/sv fibroblasts very few internalized clathrin-coated vesicles (only 5.5% (sv/sv1) or 4% (sv/sv2)) were detected (Fig. 3*B*). However, when the MVI NoI isoform was transfected into and expressed in sv/sv fibroblasts, it was possible to rescue clathrin-mediated endocytosis to roughly similar wt/wt levels (29.5%) (Fig. 3*B*). These results suggest that although sv/sv fibroblasts are able to assemble and start to form clathrin-coated pits at the plasma membrane, they are unable to further invaginate or pinch off and therefore are able to release only a small percentage of the clathrin-coated vesicles into the cell.

Transferrin Uptake in sv/sv Fibroblasts—The transferrin receptor is considered the prototype of a receptor internalized by clathrin-dependent endocytosis. To investigate whether the transferrin receptor is internalized normally in sv/sv cells that show a strong reduction in the number of clathrin-coated vesicles released into the cell, Tf-HRP internalization in sv/sv and wt/wt fibroblasts were followed in a time course uptake assay. Receptor-mediated endocytosis appeared to be more efficient in the sv/sv fibroblasts compared with wt/wt fibroblasts (Fig. 4*A*), suggesting that other endocytic mechanisms must be up-regulated to compensate for the defect in clathrin-mediated endocytosis that occurs in sv/sv fibroblasts.

To investigate which mechanisms are up-regulated in the absence of myosin VI, fluid phase HRP internalization as a marker for nonselective pinocytosis was followed in sv/sv and wt/wt fibroblasts. The internalization of the HRP enzyme appeared to be comparable in the sv/sv and wt/wt fibroblasts at all time points. This result suggests that the defect in clathrin-mediated endocytosis due to the loss of myosin VI does not up-regulate fluid phase pinocytosis to compensate (Fig. 4*B*). To investigate how the TfR is internalized, wt/wt and sv/sv fibroblasts were loaded with transferrin-Alexa-555 and labeled with anti-clathrin or anti-caveolin antibodies (Fig. 4*C*). In the immunofluorescence images in sv/sv fibroblasts, the constitutively endocytosed Tf is present in caveolae and does not co-localize with clathrin, suggesting that caveolar endocytosis is the endocytic pathway that compensates for the defect in clathrin endocytosis of transferrin receptor due to the absence of myosin VI.

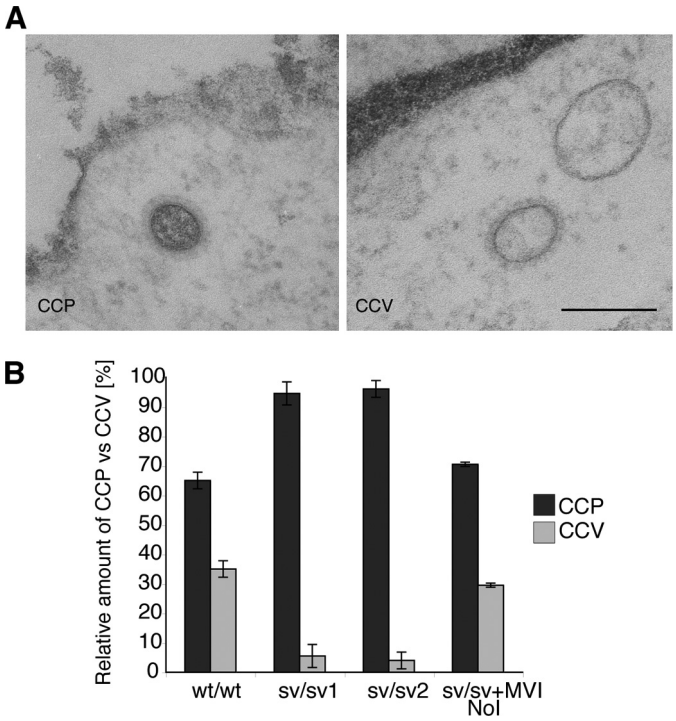

FIGURE 3. **sv/sv fibroblasts internalize only a few clathrin-coated pits as shown by ruthenium red staining.** *A*, to distinguish between a clathrin-coated pit (*CCP*) and a clathrin-coated vesicle (*CCV*), wt/wt mouse fibroblasts and two Snell's waltzer cell lines (sv/sv 1 and sv/sv 2) were fixed in the presence of the plasma membrane dye ruthenium red. EM images show a representative example of clathrin-coated pit ruthenium red-positive and -negative structures. *Bar*, 120 nm. *B*, morphometric quantitation of clathrin-coated pits and clathrin-coated vesicles present in wt/wt, sv/sv 1, sv/sv 2, and the rescue cell line (sv/sv + MVI NoI) expressing full-length myosin VI NoI. Analysis was performed on 100 CCS in two independent experiments ± S.D. The results are plotted in a histogram showing the relative amounts of clathrin-coated pits and clathrin-coated vesicles in wt/wt and sv/sv cell lines.

FIGURE 2. **Ultrastructural analysis of CCS at the plasma membrane in Snell's waltzer mouse fibroblasts.** *A*, for ultrastructural analysis of CCS at the plasma membrane, wt/wt, and sv/sv fibroblasts were processed for Epon-embedding EM. Representative electron micrographs of wt/wt and sv/sv fibroblasts indicate that sv/sv fibroblasts show a higher number of shallow CCP and a lower number of invaginated CCP or CCS without connection to the plasma membrane *Bars*: wt/wt, 200 nm; sv/sv, 500 nm. *B*, results of a morphometric analysis counting CCS in 10 cell profiles and normalized for 1000 μm of cell perimeter in four different experiments (±S.D.) are shown. For quantitation the CCS were divided into three different categories: *I*, shallow CCP; *II*, deeper invaginated CCP; and *III*, clathrin-coated pits or vesicles with no obvious connection with the plasma membrane. *C*, a histogram of the relative amounts of the three different categories of CCS in wt/wt or sv/sv fibroblasts. *D*, wt/wt and sv/sv mouse fibroblasts were transfected with GFP-tagged clathrin light chain and analyzed by epifluorescence microscope. *E*, TIRF microscopy was used to score 500 fields from each of the samples in the experiment shown in *D*, and the fields were analyzed by Volocity software to quantify the amount of clathrin structures in the two different cell lines. The *numbers* are an expression of the average intensity of GFP-clathrin in the different fields ± S.E.

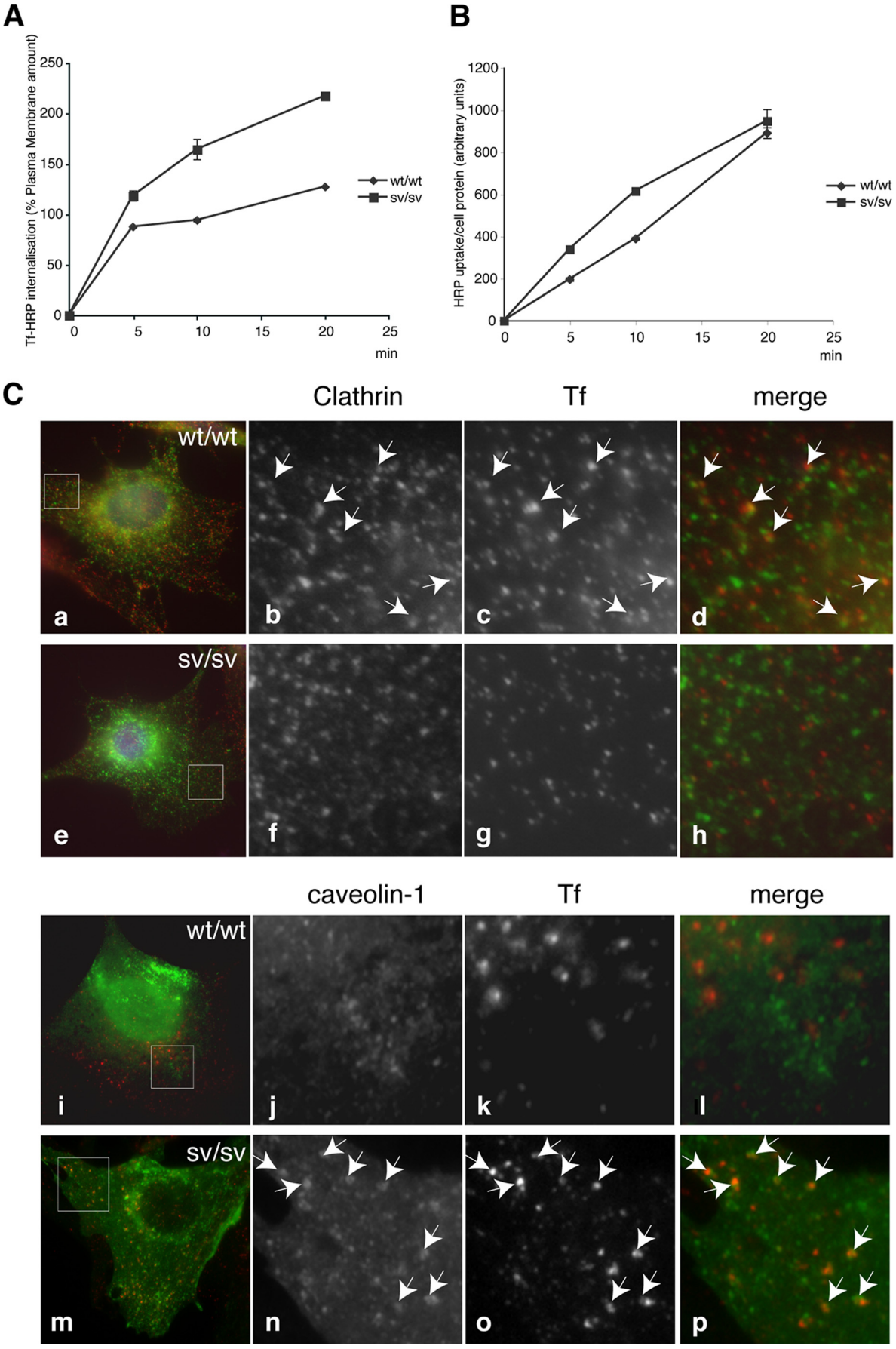
A
Tf-HRP internalisation (% Plasma Membrane amount)
250
200
150
100
50
0
0
5
10
15
20
25
min
wt/wt
sv/sv
B
HRP uptake/cell protein (arbitrary units)
1200
1000
800
600
400
200
0
0
5
10
15
20
25
min
wt/wt
sv/sv
C
Clathrin
Tf
merge
wt/wt
a
b
c
d
sv/sv
e
f
g
h
caveolin-1
Tf
merge
wt/wt
i
j
k
l
sv/sv
m
n
o
p

In sv/sv Fibroblasts the TfR Is Present in Caveolae—To further investigate whether the transferrin receptor is present in caveolae in cells lacking myosin VI, a precise EM analysis was performed on cryosections of sv/sv and wt/wt fibroblasts labeled with antibodies to the TfR. In wt/wt fibroblasts, the TfR was found, as expected, in clathrin-coated structures at the plasma membrane, whereas in sv/sv fibroblasts the receptor was associated with uncoated endocytic structures at the plasma membrane (Fig. 5*A*, *b*). Double labeling experiments with anti-caveolin-1 antibodies revealed that in sv/sv fibroblasts the receptor was present in caveolae (Fig. 5*A*, *c* and *e*). In addition, when comparing sv/sv fibroblasts with wild type, we observed a higher number of caveolae in the electron micrographs taken from sv/sv fibroblasts (Fig. 5*B*) and an increase in caveolin-1 expression by Western blotting (Fig. 5*C*).

In a morphometric quantization, the amount of gold-labeled TfR associated with clathrin-coated structures or with caveolar profiles at the plasma membrane was counted. In wt/wt cells the majority of the TfR (93%) was present in clathrin-coated structures, whereas in sv/sv fibroblasts a complete relocation of the receptor to caveolae (96%) was observed, and only 4% was still found in CCS. To test whether it was possible to restore wild type distribution of the TfR in sv/sv fibroblasts, rescue experiments were performed by expressing a GFP-myosin VI NoI isoform full-length construct in sv/sv fibroblasts. This construct was targeted to clathrin-coated structures at the plasma membrane (Figs. 1*C*, *f*, and 5*E*) and was able to rescue the wild type phenotype, with the TfR now being present in clathrin-coated structures (Fig. 5, *B* and *D*). These experiments suggest that to compensate for the defect in clathrin-mediated endocytosis caused by the loss of myosin VI, the TfR is endocytosed by a clathrin-independent, caveola-dependent pathway.

In Human Fibroblasts Expressing The Myosin VI Mutant (C442Y) the TfR Is Presents in Caveolae—Fibroblasts were obtained from an Italian family carrying a mutation in the myosin VI gene (C442Y) (28). This point mutation, near the ATP binding pocket in the motor domain, affects the motor properties of myosin VI and leads to a 10-fold increase in the ADP dissociation rate (29). To investigate whether this mutation in the motor domain affects myosin VI function in clathrin-mediated endocytosis, the TfR was immunolocalized by immunofluorescence at the EM level, and a morphometric analysis was performed as described above. In the fibroblasts expressing the myosin VI mutant (C442Y), the TfR is no longer found in the CCS, but the majority of receptor is now present in caveolae (Fig. 6, *A* and *B*). As in sv/sv fibroblasts, in myosin VI C442Y mutant fibroblasts an increase in the total number of caveolae was observed, indicating that in these mutant myosin VI-containing fibroblasts, caveola-mediated endocytosis is also up-regulated to compensate for defects in the clathrin-dependent uptake route (Fig. 6, *C* and *D*).

In Myosin VI siRNA Knockdown Cells the TfR Associates with Caveolae at the Plasma Membrane—Fibroblasts derived from the Snell's waltzer (myosin VI knock-out) mouse and mutant human myosin VI (C442Y) fibroblasts display a dramatic defect in clathrin-mediated endocytosis with a compensatory recruitment of TfR into caveolae for internalization. To verify this unexpected phenotype and to investigate whether it is linked directly to the loss of myosin VI, siRNA knockdown experiments were performed to reduce the cellular expression level of myosin VI in HeLa cells. HeLa cells were mock-treated or transfected twice with a SMARTpool of four different siRNAs specific for myosin VI. siRNA transfection reduced the expression level of myosin VI to less than 5% of the normal level as compared with mock-treated cells (Fig. 7*C*). To study the effects of myosin VI depletion on the localization of the TfR at the plasma membrane, the KD and control mock cells were fixed and processed for immuno-EM by double labeling with antibodies to caveolin-1 and the TfR (Fig. 7*A*). To analyze the distribution of the TfR at the plasma membrane, a morphometric analysis of 1000 μm of cell profiles from two independent experiments was performed. The number of gold-labeled TfR present in CCS profiles or caveolar profiles and the number of unlabeled CCS profiles or caveolar profiles at the plasma membrane were counted (Fig. 7*B*). This analysis revealed that in mock-treated cells 96% of the TfR was found in CCS profiles and only 4% in caveolar profiles, whereas in myosin VI KD cells 32% of the TfR was in CCS profiles and 68% in caveolar profiles. Moreover using the ruthenium red fixation strategy on four different HeLa stable cell lines that down-regulate myosin VI, a defect was also observed in the number of clathrin-coated vesicles internalized, similar to that found in sv/sv fibroblasts (Fig. 7*E*).

Overexpression of the Dominant Negative Myosin VI Tail Results in Smaller CCS and Recruitment of the TfR into Caveolae—In sv/sv fibroblasts and siRNA myosin VI KD cells, a relocation of the TfR from clathrin-coated structures into caveolae was observed. To use an alternative method to inhibit myosin VI function, a stable HeLa cell line overexpressing the dominant negative tail of myosin VI was used. This tail construct is able to target to clathrin-coated structures at the plasma membrane (Fig. 1*B*, *i–l*), but without the motor domain it is nonfunctional and therefore blocks the activity of endogenous myosin VI in clathrin-coated structures. The HeLa cell line expressing GFP-tagged myosin VI NoI tail was processed for immunogold labeling on cryosections and labeled with antibodies to GFP. The GFP myosin VI tail is present in clathrin-coated structures at the plasma membrane, and these CCSs appear smaller and less loaded with TfR compared with control cells (Fig. 8*A*). A 40% reduction in the size of CCSs at the plasma membrane was observed. The average size of a CCS carrying TfR is 102 $\pm$ 12 nm in control cells compared with 63 $\pm$ 12 nm in GFP-myosin VI NoI tail-expressing cells, and receptor load-

FIGURE 4. **Transferrin uptake in sv/sv fibroblasts.** wt/wt and sv/sv fibroblasts were incubated in the presence of Tf-HRP in a continuous uptake assay (*A*) or with HRP at 37 °C for different times (min) (*B*). The amount of Tf-HRP or HRP internalized was determined as described under "Experimental Procedures." The amount of Tf-HRP internalized in the continuous uptake assay is expressed as a percentage of the transferrin bound on the plasma membrane. *C*, wt/wt (*a–d* and *i–l*) and sv/sv (*e–h* and *m–p*) fibroblasts were incubated for 15 min at 37 °C with Tf-Alexa-555 (*red*) and co-localized with caveolin-1 or clathrin (*green*). The boxes in *b–d*, *f–h*, *j–l*, and *n–p* indicate the areas enlarged in adjacent panels *a*, *e*, *i*, and *m*. *Arrows* indicate examples of co-localization.

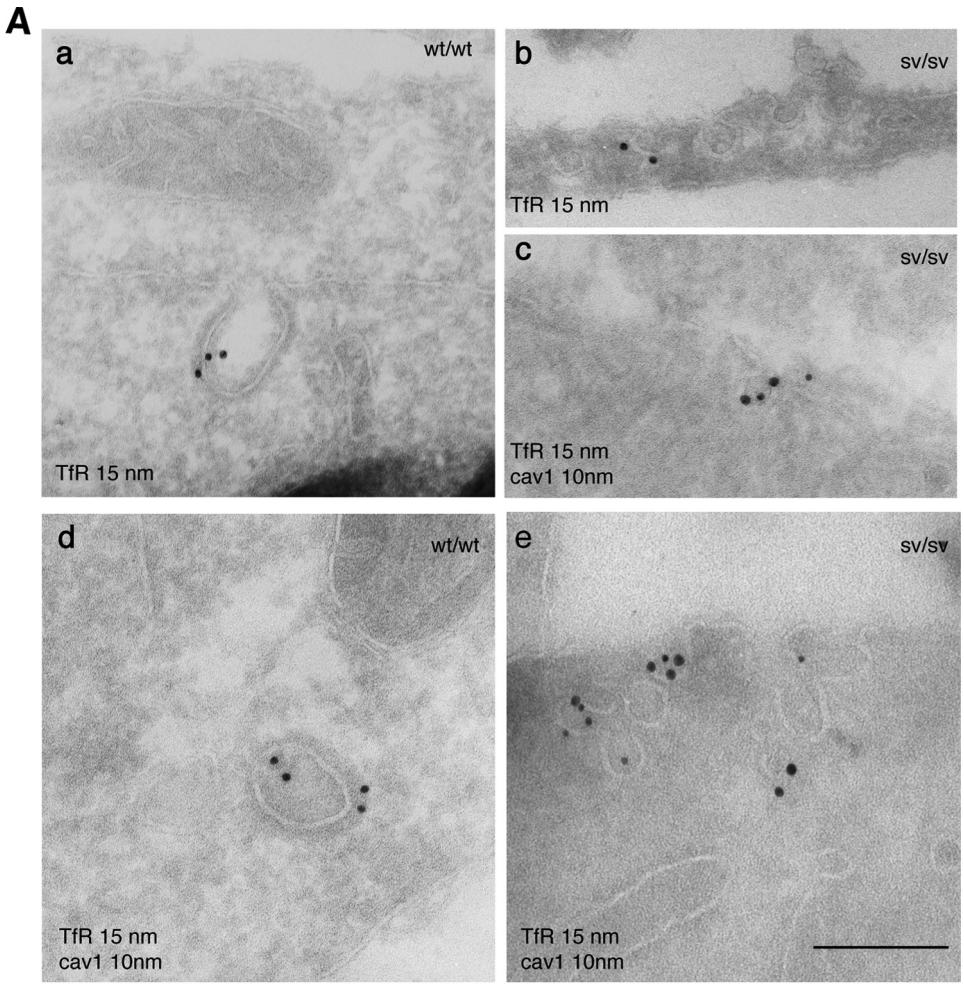

B

Number of organelles in 1000 μm of cell profile

	CCS profiles		Caveolae profiles	
	labelled	unlabelled	labelled	unlabelled
wt/wt	5.8±0.4	6.0±3.2	0.6±0	18.8±2.4
sv/sv	0.5±0.2	5.7±2.2	9.3±1.4	27.0±3.2
sv/sv +MVI NI	5.4±0.2	6.7±2.1	1.0±0	9.1±0.9

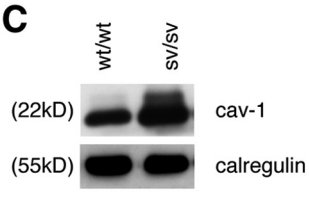

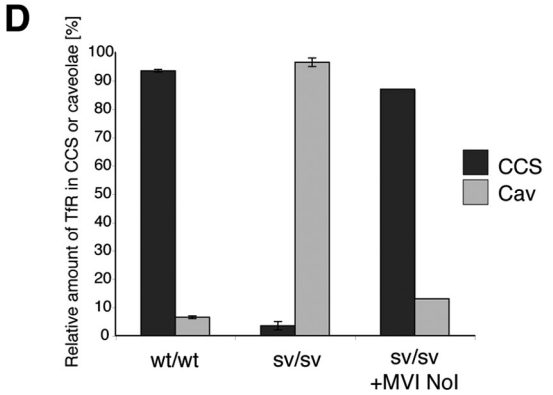

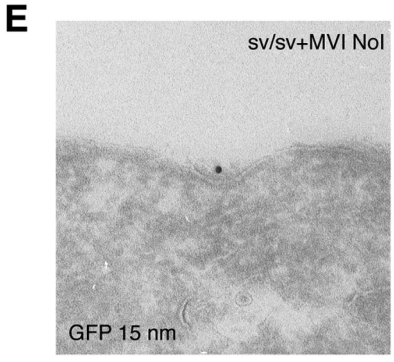

FIGURE 5. **The TfR is present in caveolae in sv/sv fibroblasts.** *A*, to visualize the TfR in endocytic structures at the plasma membrane, cryosections of wt/wt and sv/sv fibroblasts were labeled with antibodies to the TfR (*a* and *b*) and to caveolin-1 and TfR (*c*–*e*). Whereas in wt/wt fibroblasts only the TfR is present in CCS (*a* and *d*), in sv/sv fibroblasts the TfR is almost completely relocated to uncoated structures (*b*) and to caveolin-1 (*cav1*) positive structures (*c* and *e*). *Bars*: *a*, 350 nm; *b*, 350; *c*, 250 nm; *d*, 350 nm; *e*, 300 nm. *B*, to quantify these observations a morphometric analysis was carried out to determine the labeled and unlabeled organelles in 1000 μm of cell profiles. The relative amounts of TfR in CCS or caveolae in two independent experiments ± S.D. are shown. *C*, the Western blot shows an increase in caveolin-1 expression in sv/sv compared with wt/wt fibroblasts. An anti-calregulin blot is shown as the loading control. *D*, the histogram summarizes the relative amounts of TfR present in CCS or caveolae. *E*, cryosections of sv/sv fibroblasts transfected with GFP full-length myosin VI NoI (sv/sv + MVI NoI) were labeled with antibodies to GFP to localize myosin VI. The construct binds clathrin-coated structures at the plasma membrane. *Bar*, 350 nm.

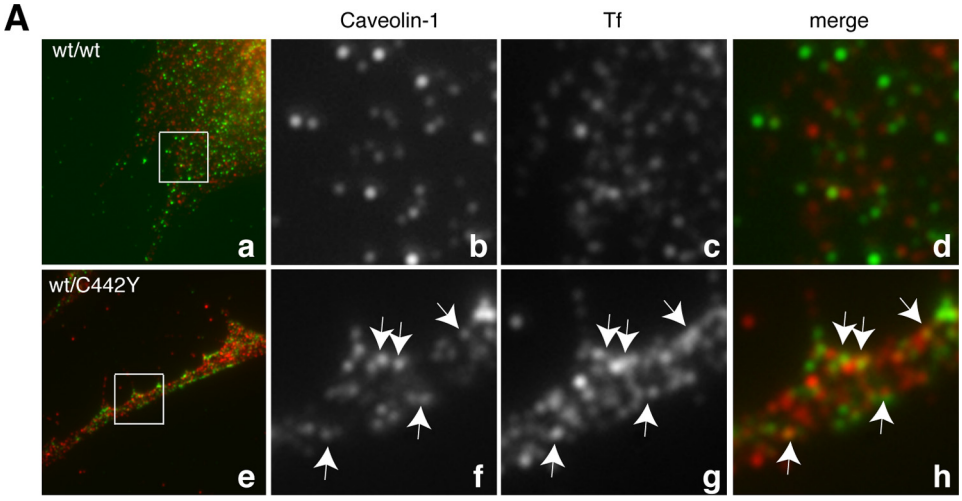

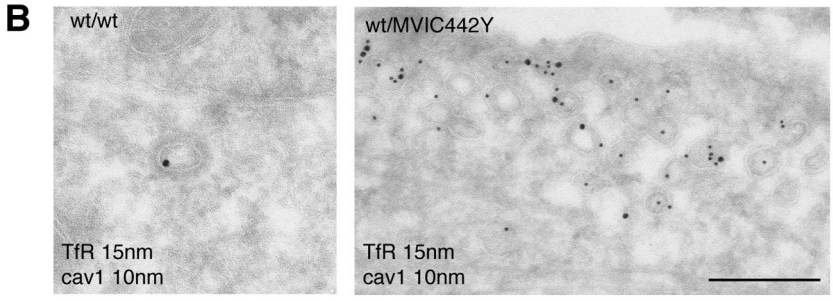

C

Number of organelles in 1000 μm of cell profile

	CCS profiles		Caveolae profiles	
	labelled	unlabelled	labelled	unlabelled
wt/wt	10.4 ± 1.3	7.8 ± 1.0	0.5 ± 0	26.9 ± 4.0
wt/MVIC442Y	3.5 ± 0.3	12.9 ± 0.6	18.3 ± 4.9	79.5 ± 49

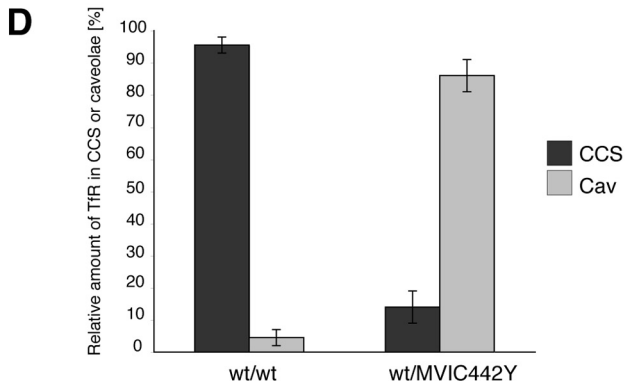

FIGURE 6. **Human fibroblasts expressing the myosin VI mutant (wt/C442Y) show a relocalization of the TfR to caveolae.** *A*, wt/wt and sv/sv fibroblasts were loaded with Tf-Alexa-555, labeled with caveolin-1, and observed by confocal microscope. As in sv/sv fibroblasts, the wt/C442Y-expressing human fibroblasts show a relocalization of transferrin to caveolae compared with the wt/wt. *B*, cryosections of human fibroblasts (wt/C442Y) and control human fibroblasts (wt/wt) were double labeled with antibodies against caveolin-1 (*cav1*) and TfR. The electron micrographs show representative fields, where the TfR is present in CCS in wt/wt cells and in caveolae in mutant wt/C442Y fibroblasts. *Bar*, 300 nm. *C*, to quantify this observation, a morphometric analysis was carried out to count the number of organelles in 1000 μm of cell profiles in human wt/wt or mutant wt/C442Y fibroblasts in two different experiments. *D*, the results of the morphometric analysis are shown in the histograms highlighting the redistribution of the TfR from CCS to caveolae in wt/C442Y fibroblasts, which carry a mutation in the motor domain in the myosin VI gene.

ing is also reduced (2.7 ± 1.3 gold particles/CCS in control and 1.8 ± 0.9 in NoI tail cells).

The reduced size and loading of CCS caused by overexpression of the myosin VI NoI tail suggests that clathrin-mediated endocytosis is less efficient. To determine where the TfR is located in these cells, a morphometric analysis was performed on cryosections of the myosin VI NoI tail-expressing cells stained with antibodies to the TfR. The number of CCS and caveolar profiles containing gold particles indicating the presence of the TfR and the number of unlabeled structures was counted in 1000 μm of cell profiles from two independent experiments (Fig. 8*D*). Whereas in control HeLa cells only 4% of the TfR was found in the caveolae, in the cells expressing the dominant negative tail, 68% of the TfR was now associated with caveolae (Fig. 8*E*). These results show that overexpression of the myosin VI NoI tail leads to defects in clathrin-coated vesicle formation and results in the association of the TfR with caveolae, thus confirming our results from sv/sv fibroblasts and siRNA myosin VI KD cells. Moreover, the smaller size of the clathrin-coated structures (with less receptor) generated by the presence of myosin VI NoI tail suggests that myosin VI might have a function in receptor loading into clathrin-coated pits.

In the Absence of Myosin VI, Does the Transferrin Receptor Relocalize Only on Caveolae or Is It Also Internalized by Caveola-mediated Endocytosis?—To determine whether loss of myosin VI induces just a relocalization of transferrin receptor onto caveolae or whether the caveolae are then able to detach from the plasma membrane to internalize the Tf receptor, the following experiments were performed on mouse fibroblasts and HeLa cells. sv/sv and wt/wt fibroblasts were treated with filipin (a cholesterol-blocking drug used normally to block caveolar uptake (4, 42, 43)), filipin and exogenous cholesterol, C8-LacCer (a lipid able to block caveolar endocytosis (40)), or Dynasore (a dynamin-blocking drug (39)) and loaded with Tf-HRP for 5 min (34, 36, 35). Filipin and LacCer treatment when used in sv/sv cells was able to reduce transferrin uptake by more than 60% (Fig. 9*A*) but had no effect on wt/wt cells. The use of exogenous cholesterol was able to rescue the effect of filipin on sv/sv fibroblasts. Dynasore

A

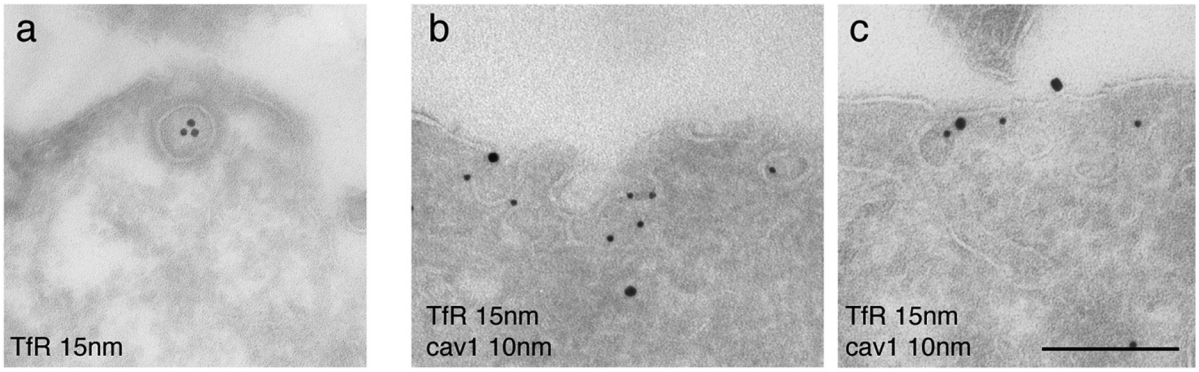

B

Number of organelles in 1000 μm of cell profile

	CCS profiles		Caveolae profiles	
	labelled	unlabelled	labelled	unlabelled
mock	24.9 ± 2.0	11.5 ± 4.3	2.2 ± 0.8	42.8 ± 21.8
MVI siRNA KD	8.3 ± 1.4	20.2 ± 3.1	15.8 ± 1.0	45.8 ± 13.8

C

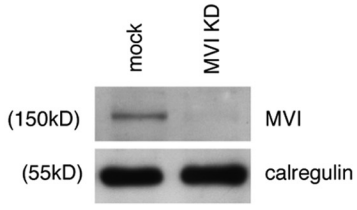

D

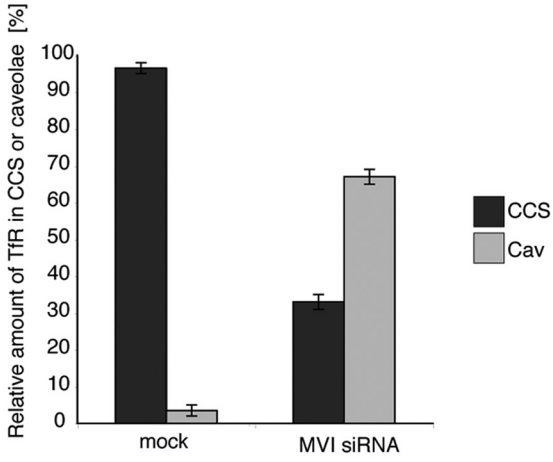

E

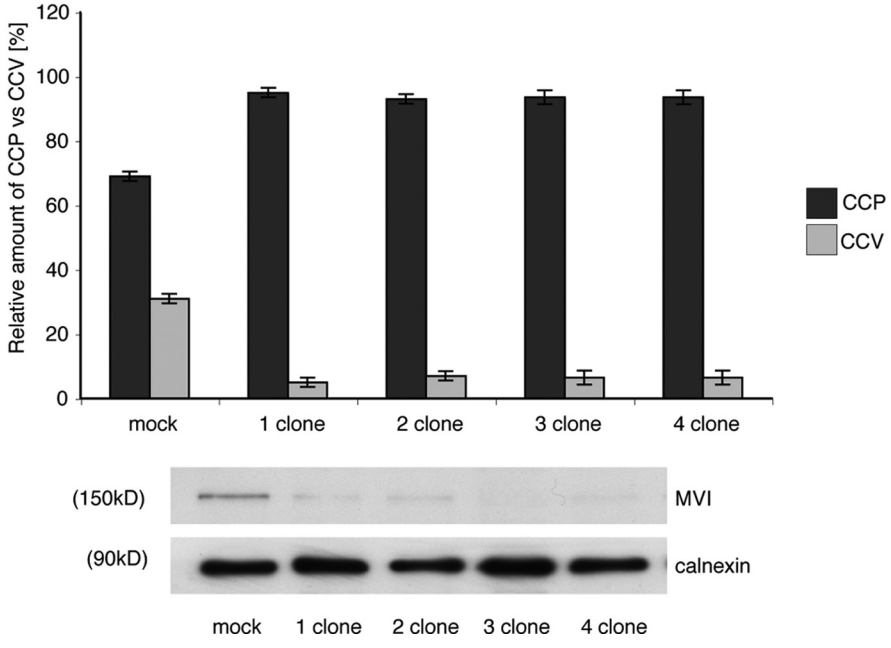

was able to block Tf internalization in both cell lines. Altogether, these results clearly show that in sv/sv fibroblasts, transferrin internalization is caveola-dependent.

To further investigate whether a loss of myosin VI induces caveola-mediated endocytosis of transferrin receptor, the effect of a reduction in caveolin-1 on transferrin internalization in mock HeLa cells or knockdown cells lacking MVI or MVI/caveolin-1 was investigated. To carry out this experiment, HeLa cells in the different conditions described above were loaded with anti-TfR antibody for 5 min and fixed for immunogold labeling on cryosections. EM morphometric analysis was performed by counting the amount of receptors still at the plasma membrane or already internalized inside the cell. The amounts of TfR internalized in cells lacking MVI and caveolin-1 were strongly delayed (Fig. 9*B*).

The same experiment was repeated using a biochemical approach to confirm the morphometric data. HeLa cells, mock-treated or treated with siRNAs to knock down both myosin VI and caveolin-1 and to double knock down myosin VI and caveolin-1, were loaded with Tf-HRP in a time course uptake. The amount of Tf-HRP internalized (detected as HRP enzyme activity) in myosin VI or caveolin-1 siRNA KD cells at all time points is comparable with the uptake in mock cells, whereas the uptake appears to be severely compromised in double caveolin-1/myosin VI KD cells (Fig. 9*E*). These results demonstrate that caveola-mediated endocytosis is the endocytic pathway used for transferrin receptor uptake in cells lacking myosin VI.

Finally, HRP uptake was analyzed in HeLa cells mock-transfected or treated with siRNAs to knock down myosin VI or caveolin-1 or myosin VI/caveolin-1 to determine whether under these conditions fluid phase pinocytosis was affected. In all four of these different HeLa cells, HRP uptake occurred with equal efficiency, supporting the results that caveola-dependent endocytosis is the main pathway up-regulated when myosin VI is absent (Fig. 9*F*). In conclusion, these results show that in mouse fibroblasts and HeLa cells in the absence of myosin VI, clathrin-mediated endocytosis is impaired, and instead the caveola-dependent endocytic pathway is used for internalization of the transferrin receptor.

When Myosin VI Is Absent, Clathrin Adaptor Protein AP-2 Follows the Transferrin Receptor to Caveolae—A number of published papers have shown that loss of AP-2 induces a complete block in TfR uptake (44, 45); thus the transferrin receptor needs AP-2 to be internalized normally. From the results described above, loss of the myosin VI NoI isoform induces a block in clathrin-mediated endocytosis without a block in transferrin receptor endocytosis. The only explanation can be that loss of myosin VI also induces a relocalization of clathrin adaptor protein AP-2 to caveolae following and allowing receptor internalization.

To address this important point, the following experiments were performed. wt/wt and sv/sv fibroblasts were fixed, labeled with antibodies to anti-caveolin-1 and anti-AP-2, and analyzed by TIRF microscope; they showed an increase of co-localization between caveolin-1 and AP-2 in sv/sv fibroblasts (Fig. 10*A*). The same experiment was performed by immuno-EM, and similar results were observed (Fig. 10*B*). EM morphometric analysis shows that there is a relocalization of AP-2 in caveolae in Snell's waltzer fibroblasts compared with the wild type. Moreover AP-2 relocalized back into clathrin-coated structures when myosin VI NoI isoform expression was restored (sv/sv + NoI) (Fig. 10, *C* and *D*).

These results clearly show that loss of myosin VI NoI isoform induces caveolar endocytosis of the transferrin receptor and that clathrin adaptor protein AP-2 follows the receptor in this alternative endocytic pathway. These results imply that the percentage of co-localization of AP-2 and TfR in sv/sv and wt/wt fibroblasts must remain quite similar in both conditions. To verify this hypothesis, sv/sv and wt/wt fibroblasts were loaded with Tf-Alexa-555 and labeled with anti-AP-2 antibody. Software analysis of TIRF microscopy images showed a similar percentage of co-localization between sv/sv and wt/wt. These results show not only that lack of myosin VI induces a relocalization of the transferrin receptor from clathrin to caveolae but also that clathrin adaptor protein AP-2, necessary for internalization of the receptor, follows the receptor to caveolae.

DISCUSSION

In this study the endocytic uptake route of the TfR was examined in cells missing or expressing mutant forms of myosin VI NoI isoform. It was observed that in these cells without a functional myosin VI, fewer clathrin-coated vesicles were released from the plasma membrane. Using electron microscopy it was demonstrated that the TfR was no longer present in clathrin-coated structures at the plasma membrane, but a dramatic relocalization into caveolae was shown.

The cells that were examined in the present study did not express the large insert isoform. This isoform is in some cases correlated with clathrin-mediated endocytosis (9, 12),

FIGURE 7. **Depletion of myosin VI in HeLa cells using siRNA knockdown relocates the TfR from CCS to caveolae.** HeLa cells were either mock-transfected or transfected twice with siRNAs specific to myosin VI or to myosin VI and caveolin-1. *A*, mock-treated HeLa cells and KD cells were loaded with mouse anti-TfR antibody at 37 °C before fixation and processing for immuno-EM. Ultrathin cryosections were double labeled with anti-caveolin-1 and rabbit anti-mouse antibodies to visualize TfR. Representative electron micrographs show the localization of the TfR in CCS in control cells and co-localization with caveolin-1 in myosin VI KD cells. Bars: *a*, 250 nm; *b*, 200 nm; *c*, 200 nm. *B*, to quantify this observation a morphometric analysis was carried out to determine the numbers of TfR-labeled and unlabeled organelles in 1000 μm of cell profiles of mock-treated and myosin VI KD cells. The relative amounts of TfR in CCS or caveolae in two independent experiments ± S.D. are shown. *C*, the amount of myosin VI in the cells is shown in the Western blot with calregulin as a loading control. *D*, the histogram shows the relative amounts of TfR in caveolae and CCS in mock and siRNA MVI KD cells. *E*, HeLa cells were transfected with SureSilencing™ myosin VI small hairpin RNA plasmids (SuperArray-Bioscience Corp.) carrying the puromycin resistance gene. The puromycin resistance HeLa cell population was subcloned, and four clones expressing no significant level of myosin VI were selected. The four clones and the negative control were fixed under steady state conditions using the same labeling protocol with ruthenium red/glutaraldehyde described previously for mouse fibroblasts. All four HeLa clones that down-regulate myosin VI show a 5–6-fold reduction in clathrin-coated vesicle (*CCV*) internalization compared with the negative control. *CCP*, clathrin-coated pits.

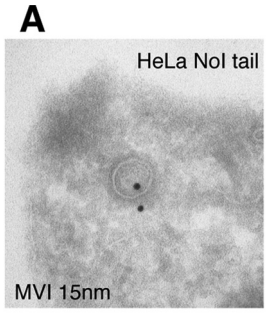

B

	Diameter [nm]	loading (N. TfR/CCS)
HeLa CTR	102 ±12	2.7±1.3
HeLa NoI tail	63±12	1.8±0.9

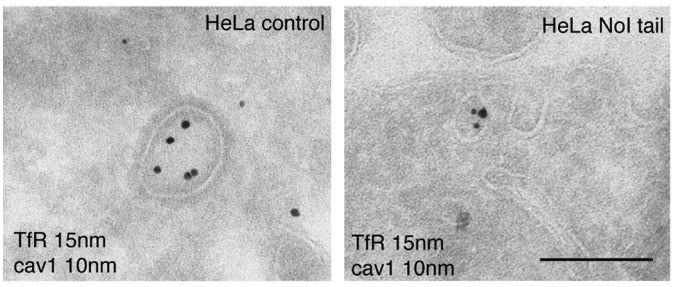

D

Number of organelles in 1000 μm of cell profile

	CCS profiles		Caveolae profiles	
	labelled	unlabelled	labelled	unlabelled
HeLa control	17.6 ± 3.6	8.7 ± 4.3	1.4 ± 0.4	28.5 ± 7.1
HeLa NoI tail	11.3 ± 0.7	14.3 ± 2.1	37.4 ±13.9	66.5 ±18.8

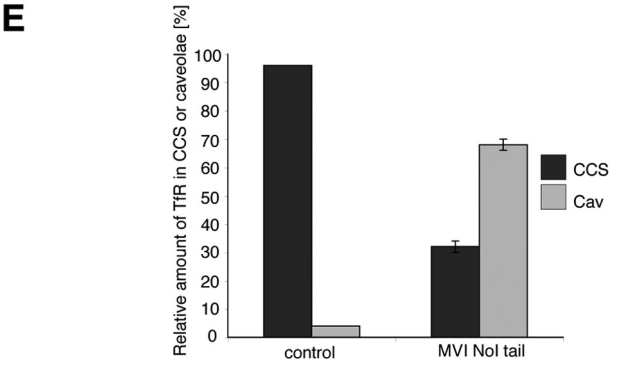

FIGURE 8. **Overexpression of the dominant negative myosin VI NoI tail leads to defective clathrin-coated vesicles with relocalization of TfR to the caveolae.** *A*, HeLa cells expressing GFP-tagged myosin VI NoI tail and control cells were processed for immuno-EM. The picture shows a representative field of HeLa cells expressing GFP-tagged myosin VI NoI tail. Ultrathin cryosections labeled with GFP antibodies show localization of GFP-myosin VI NoI tail in CCS at the plasma membrane. *Bar*, 200 nm. *B*, the size of CCS (diameter) and the transferrin receptor loading was measured in 70 cell profiles of control (*CTR*) and myosin VI NoI tail-expressing cells. *C*, cryosections of control and myosin VI NoI tail-expressing cells were double labeled with anti-caveolin-1 (*cav1*) and anti-TfR antibodies. Representative electron micrographs highlight localization of the TfR in caveolae in myosin VI NoI tail-expressing cells. *Bar*, 200 nm. *D*, morphometric quantitation was performed on cryosections of control and myosin VI NoI tail-expressing cells labeled with antibodies against caveolin-1 and TfR. *E*, the histograms represent the relative amount of Tf receptor localized on clathrin-coated structures *versus* caveolae.

whereas in some other cases it is shown not to have major or minor co-localization with clathrin adaptor AP-2 (16). Moreover the binding sequences with Dab2 and PIP_2, necessary for clathrin-coated structure binding, are conserved in all myosin VI isoforms (12). In the present study the defect in endocytosis observed in the absence of myosin VI was rescued by re-expressing the NoI isoform, which shows definitively that this isoform is correlated with clathrin-mediated endocytosis. These EM studies show in cells that lack or express a defective myosin VI NoI isoform that there is a strong co-localization between the TfR and caveolin-1, suggesting that the caveolin-dependent uptake route is mobilized. Indeed, in sv/sv and myosin VI C442Y fibroblasts, there was an increase in the number of caveolae in the electron micrographs (Figs. 5*B*, 6*C*, and 8*D*), and an overexpression of caveolin-1 by Western blotting was observed (Fig. 5*C*).

Live cell microscopy has shown that caveolae are stable structures at the plasma membrane with a slow rate of turnover. However, mobility and turnover can be increased by using okadaic acid (a phosphatase inhibitor) or through the addition of glycosphingolipids and cholesterol (46–49). In this study it would appear that the caveola-dependent endocytic pathway is able to internalize plasma membrane receptors such as TfR with a speed and efficiency comparable with that of clathrin-mediated endocytosis (Figs. 4*A* and 9, *C* and *E*).

The mobilization of alternative endocytic pathways to increase bulk endocytosis has been reported in cells expressing a temperature-sensitive mutant of dynamin that inhibits clathrin and caveola-dependent endocytosis (32, 34, 50), and in caveolin-1 null mouse cell lines, caveolin-independent endocytic pathways are up-regulated (51, 52). Indeed, the flexibility of cell surface receptors to be endocytosed by more then one mechanism underlines the cross-talk and interplay between different endocytic pathways. For example, GLUT4 is mostly endocytosed by a clathrin-independent pathway in unstimulated adipocytes, but in the presence of insulin this receptor is endocytosed in a clathrin-dependent manner (53). The EGFR has also been reported to take different routes to enter the cell. Clathrin-mediated endocytosis is the established uptake route for the EGFR; however, when cells are stimulated with high concentrations of growth factor, the receptor becomes ubiquitinated and is endocytosed through a clathrin-independent pathway (4). Similarly, in cells under decorin stimulation (5) or oxidative stress (6), the EGFR is endocytosed by a clathrin-independent pathway. Interleukin 2 and its receptor can also be internalized by an alternative rapid endocytic pathway when clathrin-dependent endocytosis is inhibited (54, 55). Moreover the small molecule iron transport inhibitor ferristatin promotes transferrin receptor internalization by an alternative clathrin/dynamin-independent, cholesterol-dependent, endocytic pathway (8).

The ability of cell surface receptors to use more than one endocytic pathway enables sv/sv fibroblasts to utilize an alternative uptake route to compensate for the defect in clathrin-mediated endocytosis. In sv/sv fibroblasts the TfR is found in caveolae, which are an abundant feature at the plasma membrane in fibroblasts, adipocytes, and endothelial cells. However, unlike clathrin, caveolin is not expressed in all cell types and tissues; for example, caveolae are not present at the plasma membrane in the apical domains of Madin-Darby canine kidney cells and Caco-2 cells (56). In the Snell's waltzer mouse defects in clathrin-mediated endocytosis of the cystic

fibrosis transmembrane regulator at the apical domain of enterocyte brush border cells have been reported (27). Interestingly, the apical domains of enterocyte brush border cells lack caveolae, which may compensate for the loss of the clathrin-dependent internalization pathway (57). Moreover, in this study it also has been shown that clathrin adaptor AP-2 is recruited into caveolae following the transferrin receptor. It is known that AP-2 needs a plasma membrane receptor and the lipid PIP_2 to

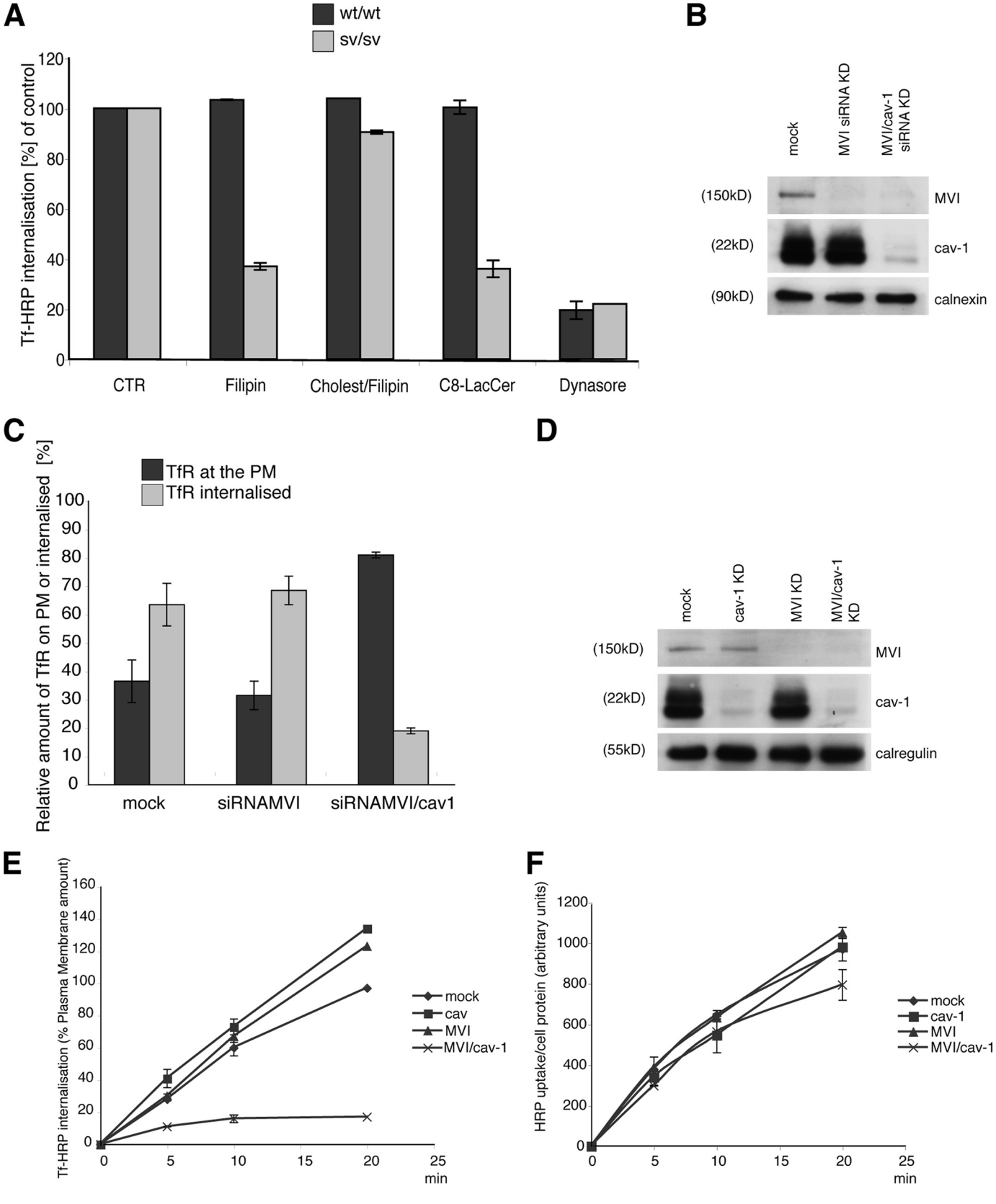

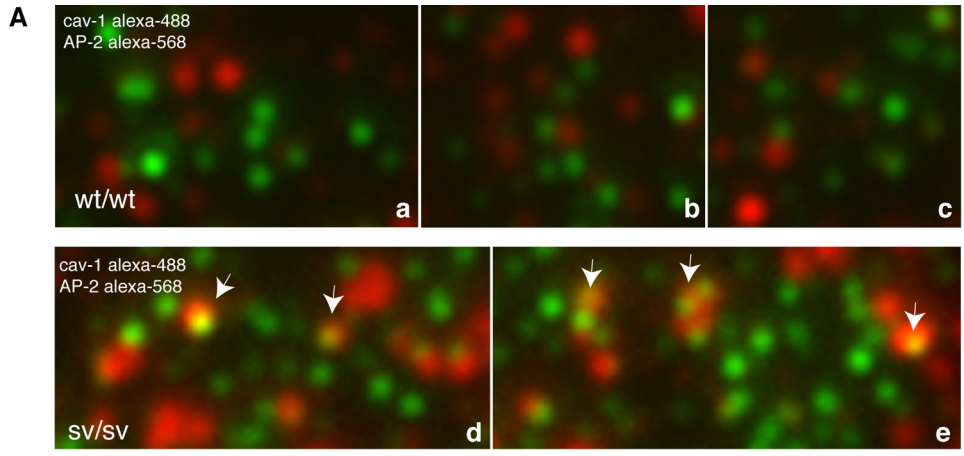

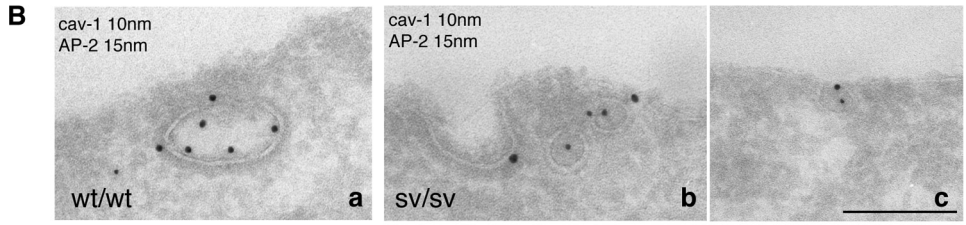

C

Number of organelles in 1000 µm of cell profile

	CCS profiles		Caveolae profiles	
	labelled	unlabelled	labelled	unlabelled
wt/wt	7.4±0	3.7±0.2	0±0	18.7±6.1
sv/sv	4.1±0.3	3.7±0.3	2.1±0.3	24.1±0.1
sv/sv +MVI NoI	7.7±0.3	3.3±0.1	0.08±0.08	14.5±0.7

D

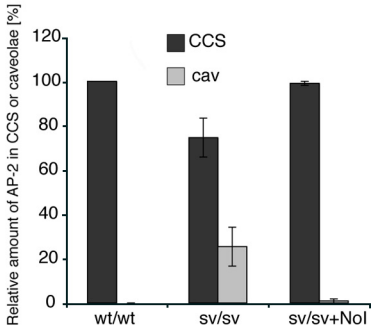

E

	% of colocalisation AP-2-Tf
wt/wt	41.6 ± 1.05
sv/sv	43.03 ± 0.6

FIGURE 10. **The clathrin adaptor protein, AP-2, relocalizes into caveolae when myosin VI is lost.** *A*, wt/wt and sv/sv fibroblasts were fixed under steady state condition and labeled with anti-caveolin-1 anti-AP-2 antibodies. The samples were observed by TIRF microscopy. The figure shows different fields of the wt/wt (*a–c*) and sv/sv (*d* and *e*) labeled samples. In sv/sv images, AP-2 co-localizes with caveolin-1 (*arrows*), whereas in the wt/wt images they are completely independent. *B*, similar experiment was performed by immuno-EM. Cryosections of wt/wt (*a*) and sv/sv (*b* and *c*) fibroblasts were double labeled with anti-caveolin-1 (*cav-1*) and anti-AP-2 antibodies. Using this different technique a relocalization of the clathrin adaptor protein AP-2 in caveolae was also observed. *Bars*: *a*, 300 nm; *b*, 200 nm; *c*, 300 nm. *C*, to quantify this observation a morphometric analysis was carried out on AP-2 labeling in CCS or caveolae organelles in 1000 μm of cell profiles of wt/wt and sv/sv fibroblasts. AP-2 localization on clathrin-coated structures was restored when the myosin VI NoI isoform was re-expressed in sv/sv fibroblasts. *D*, the relative amounts of AP-2 in CCS or caveolae in two independent experiments ± S.D. are shown. *E*, wt/wt and sv/sv fibroblasts were loaded with Tf-Alexa-555 and labeled with anti-AP-2 antibody. 500 fields of each sample were scanned by TIRF microscope and analyzed by Volocity software. The percentage of co-localization between AP-2 and transferrin does not change between wt/wt and sv/sv fibroblasts, revealing that the clathrin adaptor follows the transferrin receptor whether it is internalized by clathrin or caveolae.

bind membranes; the K_D of binding of AP-2 to PIP_2 and a receptor with the sorting signal $YXX\phi$, such as transferrin receptor, is 500 μM (20). Caveolae are enriched in the lipid PIP_2 (58, 59). Thus, caveolae represent the best candidate for internalizing transferrin receptor when the clathrin-mediated endocytosis is not available.

Why does AP-2 bind to the PIP_2 in caveolae and not in clathrin-coated structures when myosin VI is lost? It is known that myosin VI binds with high efficiency PIP_2 (12), so the role of the myosin VI NoI isoform could be to bind and recruit PIP_2 inside the dedicated "hot spots" on the plasma membrane for clathrin-coated nucleation and internalization (60, 61). Without myosin VI, it is possible that the clathrin-coated structures would be relatively poor in PIP_2 and thus unable to recruit enough AP-2 for a normal endocytosis. Under this condition, AP-2 and the receptor are recruited to another endocytic structure enriched in PIP_2, namely caveolae. Further investigations will be necessary to prove this model.

The data presented in this article show a severe but not a complete block in clathrin-mediated endocytosis. Why are some clathrin-coated vesicles still able to leave the plasma membrane? Probably in some hot spots the amount of PIP_2 is enough to assemble an almost "normal" clathrin-coated structure. These clathrin-coated vesicles that leave the plasma membrane are probably not fully loaded with PIP_2-AP-2-receptor but still are able to leave the plasma membrane. In HeLa cell stably transfected with the dominant negative myosin VI NoI tail, a reduc-

FIGURE 9. **The transferrin receptor is internalized by caveolae when myosin VI is lost.** *A*, sv/sv and wt/wt cells were serum-starved and incubated with filipin (1.2 μg/ml), cholesterol/filipin (1 mM and 1.2 μg/ml), C8-LacCer (10 μm), and Dynasore (120 mM), and the Tf-HRP uptake protocol described under "Experimental Procedures" was performed. *CTR*, control. *B*, HeLa cells were transfected twice with siRNA specific to myosin VI or myosin VI and caveolin-1 (*cav-1*). The amount of myosin VI or myosin VI and caveolin-1 in the cells is shown in the Western blot with calnexin as the loading control. *C*, these HeLa mock cells or cells lacking myosin VI or myosin VI and caveolin-1 were loaded with anti-TfR antibody for 5 min and fixed for immunogold labeling on cryosections. Morphometric analysis was performed by counting the amount of receptors still at the plasma membrane (*PM*) or already internalized inside the cell. *TIR*, total internal reflections. *D*, HeLa cells were transfected twice with siRNA specific to myosin VI, caveolin-1, or myosin VI and caveolin-1. The amounts of myosin VI and caveolin-1 in the mock and knockdown cells are shown on a Western blot, and calregulin is used as the loading control. *E*, HeLa cells analyzed in *D* were loaded with Tf-HRP in the continuous uptake assay for different times (min). The enzyme activity of Tf-HRP internalized at the different time points and in the different mock and knockdown cells was measured. The graph shows the amount of Tf-HRP internalized in mock, caveolin-1, myosin VI, and myosin VI/caveolin-1 siRNA KD cells expressed as a percentage of the plasma membrane amount of transferrin. *F*, HeLa cells analyzed in *D* were loaded with the fluid phase marker HRP. The graph shows the enzyme activity at different time points in the different mock and knockdown cells.

tion in the size and loading of clathrin-coated vesicles was observed.

It is also possible that another, thus far unidentified motor protein may be able to partially compensate for the absence of myosin VI and lead to low levels of clathrin-mediated endocytosis. An obvious conclusion to be drawn from these results is that because endocytosis is an absolutely essential cell function, it is likely that there is a significant level of redundancy in both humans and mice so that other endocytic pathways are able to compensate, at least partially, for a defect in the clathrin-mediated endocytic pathway.

Acknowledgments—I thank Dr. Folma Buss and Dr. John Kendrick-Jones for reagents and for help and advice and Prof. Paul Luzio for support; Dr. Jan Willem Slot, Dr. Hans J. Geuze, and Dr. George Posthuma for support and critical reading of the manuscript; Prof. Carlo Tacchetti and Sue D. Arden for help and critical suggestions; Dr. Andrew A. Peden and Dr. Elena Miranda for help in transferrin uptake assays; Mark Bowen and Matthew Gratian for help in confocal analysis; Jason Cooper for the statistics; Dr. Salvatore Melchionda and Angelo Notarangelo for the MVI C442Y primary cells line from the Italian family; and Prof. Karen B. Avraham for the Snell's waltzer mice.

REFERENCES

1. Conner, S. D., and Schmid, S. L. (2003) *J. Cell Biol.* **162,** 773–779
2. Mayor, S., and Pagano, R. E. (2007) *Nat. Rev. Mol. Cell Biol.* **8,** 603–612
3. Orth, J. D., Krueger, E. W., Weller, S. G., and McNiven, M. A. (2006) *Cancer Res.* **66,** 3603–3610
4. Sigismund, S., Woelk, T., Puri, C., Maspero, E., Tacchetti, C., Transidico, P., Di Fiore, P. P., and Polo, S. (2005) *Proc. Natl. Acad. Sci. U.S.A.* **102,** 2760–2765
5. Zhu, J. X., Goldoni, S., Bix, G., Owens, R. T., McQuillan, D. J., Reed, C. C., and Iozzo, R. V. (2005) *J. Biol. Chem.* **280,** 32468–32479
6. Khan, E. M., Heidinger, J. M., Levy, M., Lisanti, M. P., Ravid, T., and Goldkorn, T. (2006) *J. Biol. Chem.* **281,** 14486–14493
7. Sigismund, S., Argenzio, E., Tosoni, D., Cavallaro, E., Polo, S., and Di Fiore, P. P. (2008) *Dev. Cell* **15,** 209–219
8. Horonchik, L., and Wessling-Resnick, M. (2008) *Chem. Biol.* **15,** 647–653
9. Buss, F., Arden, S. D., Lindsay, M., Luzio, J. P., and Kendrick-Jones, J. (2001) *EMBO J.* **20,** 3676–3684
10. Morris, S. M., Arden, S. D., Roberts, R. C., Kendrick-Jones, J., Cooper, J. A., Luzio, J. P., and Buss, F. (2002) *Traffic* **3,** 331–341
11. Buss, F., Luzio, J. P., and Kendrick-Jones, J. (2002) *Traffic* **3,** 851–858
12. Spudich, G., Chibalina, M. V., Au, J. S., Arden, S. D., Buss, F., and Kendrick-Jones, J. (2007) *Nat. Cell Biol.* **9,** 176–183
13. Biemesderfer, D., Mentone, S. A., Mooseker, M., and Hasson, T. (2002) *Am. J. Physiol. Renal Physiol.* **282,** F785–F794
14. Wells, A. L., Lin, A. W., Chen, L. Q., Safer, D., Cain, S. M., Hasson, T., Carragher, B. O., Milligan, R. A., and Sweeney, H. L. (1999) *Nature* **401,** 505–508
15. Au, J. S., Puri, C., Ihrke, G., Kendrick-Jones, J., and Buss, F. (2007) *J. Cell Biol.* **177,** 103–114
16. Dance, A. L., Miller, M., Seragaki, S., Aryal, P., White, B., Aschenbrenner, L., and Hasson, T. (2004) *Traffic* **5,** 798–813
17. Aschenbrenner, L., Lee, T., and Hasson, T. (2003) *Mol. Biol. Cell* **14,** 2728–2743
18. Inoue, A., Sato, O., Homma, K., and Ikebe, M. (2002) *Biochem. Biophys. Res. Commun.* **292,** 300–307
19. Yun, M., Keshvara, L., Park, C. G., Zhang, Y. M., Dickerson, J. B., Zheng, J., Rock, C. O., Curran, T., and Park, H. W. (2003) *J. Biol. Chem.* **278,** 36572–36581
20. Höning, S., Ricotta, D., Krauss, M., Späte, K., Spolaore, B., Motley, A., Robinson, M., Robinson, C., Haucke, V., and Owen, D. J. (2005) *Mol. Cell* **18,** 519–531
21. Inoue, T., Kon, T., Ohkura, R., Yamakawa, H., Ohara, O., Yokota, J., and Sutoh, K. (2008) *Genes Cells* **13,** 483–495
22. Chibalina, M. V., Seaman, M. N., Miller, C. C., Kendrick-Jones, J., and Buss, F. (2007) *J. Cell Sci.* **120,** 4278–4288
23. Avraham, K. B., Hasson, T., Steel, K. P., Kingsley, D. M., Russell, L. B., Mooseker, M. S., Copeland, N. G., and Jenkins, N. A. (1995) *Nat. Genet.* **11,** 369–375
24. Deol, M. S., and Green, M. C. (1966) *Genet. Res.* **8,** 339–345
25. Self, T., Sobe, T., Copeland, N. G., Jenkins, N. A., Avraham, K. B., and Steel, K. P. (1999) *Dev. Biol.* **214,** 331–341
26. Osterweil, E., Wells, D. G., and Mooseker, M. S. (2005) *J. Cell Biol.* **168,** 329–338
27. Ameen, N., and Apodaca, G. (2007) *Traffic* **8,** 998–1006
28. Melchionda, S., Ahituv, N., Bisceglia, L., Sobe, T., Glaser, F., Rabionet, R., Arbones, M. L., Notarangelo, A., Di Iorio, E., Carella, M., Zelante, L., Estivill, X., Avraham, K. B., and Gasparini, P. (2001) *Am. J. Hum. Genet.* **69,** 635–640
29. Sato, O., White, H. D., Inoue, A., Belknap, B., Ikebe, R., and Ikebe, M. (2004) *J. Biol. Chem.* **279,** 28844–28854
30. Ahmed, Z. M., Morell, R. J., Riazuddin, S., Gropman, A., Shaukat, S., Ahmad, M. M., Mohiddin, S. A., Fananapazir, L., Caruso, R. C., Husnain, T., Khan, S. N., Riazuddin, S., Griffith, A. J., Friedman, T. B., and Wilcox, E. R. (2003) *Am. J. Hum. Genet.* **72,** 1315–1322
31. Puri, C., Tosoni, D., Comai, R., Rabellino, A., Segat, D., Caneva, F., Luzzi, P., Di Fiore, P. P., and Tacchetti, C. (2005) *Mol. Biol. Cell* **16,** 2704–2718
32. Damke, H., Baba, T., Warnock, D. E., and Schmid, S. L. (1994) *J. Cell Biol.* **127,** 915–934
33. Rabouille, C., Misteli, T., Watson, R., and Warren, G. (1995) *J. Cell Biol.* **129,** 605–618
34. Damke, H., Baba, T., van der Bliek, A. M., and Schmid, S. L. (1995) *J. Cell Biol.* **131,** 69–80
35. Parton, R. G., Joggerst, B., and Simons, K. (1994) *J. Cell Biol.* **127,** 1199–1215
36. Sakai, T., Yamashina, S., and Ohnishi, S. (1991) *J. Biochem.* **109,** 528–533
37. Tosoni, D., Puri, C., Confalonieri, S., Salcini, A. E., De Camilli, P., Tacchetti, C., and Di Fiore, P. P. (2005) *Cell* **123,** 875–888
38. Imelli, N., Meier, O., Boucke, K., Hemmi, S., and Greber, U. F. (2004) *J. Virol.* **78,** 3089–3098
39. Abban, C. Y., Bradbury, N. A., and Meneses, P. I. (2008) *Am. J. Ther.* **15,** 304–311
40. Singh, R. D., Holicky, E. L., Cheng, Z. J., Kim, S. Y., Wheatley, C. L., Marks, D. L., Bittman, R., and Pagano, R. E. (2007) *J. Cell Biol.* **176,** 895–901
41. Arden, S. D., Puri, C., Au, J. S., Kendrick-Jones, J., and Buss, F. (2007) *Mol. Biol. Cell* **18,** 4750–4761
42. Shigematsu, S., Watson, R. T., Khan, A. H., and Pessin, J. E. (2003) *J. Biol. Chem.* **278,** 10683–10690
43. Torgersen, M. L., Skretting, G., van Deurs, B., and Sandvig, K. (2001) *J. Cell Sci.* **114,** 3737–3747
44. Motley, A., Bright, N. A., Seaman, M. N., and Robinson, M. S. (2003) *J. Cell Biol.* **162,** 909–918
45. Conner, S. D., and Schmid, S. L. (2002) *J. Cell Biol.* **156,** 921–929
46. Kurzchalia, T. V., and Parton, R. G. (1996) *FEBS Lett.* **389,** 52–54
47. Parton, R. G. (2003) *Nat. Rev. Mol. Cell Biol.* **4,** 162–167
48. Sharma, D. K., Brown, J. C., Choudhury, A., Peterson, T. E., Holicky, E., Marks, D. L., Simari, R., Parton, R. G., and Pagano, R. E. (2004) *Mol. Biol. Cell* **15,** 3114–3122
49. Hommelgaard, A. M., Roepstorff, K., Vilhardt, F., Torgersen, M. L., Sandvig, K., and van Deurs, B. (2005) *Traffic* **6,** 720–724
50. Damke, H., Gossen, M., Freundlieb, S., Bujard, H., and Schmid, S. L. (1995) *Methods Enzymol.* **257,** 209–220
51. Damm, E. M., Pelkmans, L., Kartenbeck, J., Mezzacasa, A., Kurzchalia, T., and Helenius, A. (2005) *J. Cell Biol.* **168,** 477–488
52. Kirkham, M., Fujita, A., Chadda, R., Nixon, S. J., Kurzchalia, T. V., Sharma, D. K., Pagano, R. E., Hancock, J. F., Mayor, S., and Parton, R. G. (2005) *J. Cell Biol.* **168,** 465–476
53. Blot, V., and McGraw, T. E. (2006) *EMBO J.* **25,** 5648–5658

54. Subtil, A., Hémar, A., and Dautry-Varsat, A. (1994) *J. Cell Sci.* **107,** 3461–3468
55. Lamaze, C., Dujeancourt, A., Baba, T., Lo, C. G., Benmerah, A., and Dautry-Varsat, A. (2001) *Mol. Cell* **7,** 661–671
56. Vogel, U., Sandvig, K., and van Deurs, B. (1998) *J. Cell Sci.* **111,** 825–832
57. Danielsen, E. M., and Hansen, G. H. (2006) *Mol. Membr. Biol.* **23,** 71–79
58. Pike, L. J., and Casey, L. (1996) *J. Biol. Chem.* **271,** 26453–26456
59. Fujita, A., Cheng, J., Tauchi-Sato, K., Takenawa, T., and Fujimoto, T. (2009) *Proc. Natl. Acad. Sci. U.S.A.* **106,** 9256–9261
60. Gaidarov, I., Santini, F., Warren, R. A., and Keen, J. H. (1999) *Nat. Cell Biol.* **1,** 1–7
61. Ehrlich, M., Boll, W., Van Oijen, A., Hariharan, R., Chandran, K., Nibert, M. L., and Kirchhausen, T. (2004) *Cell* **118,** 591–605